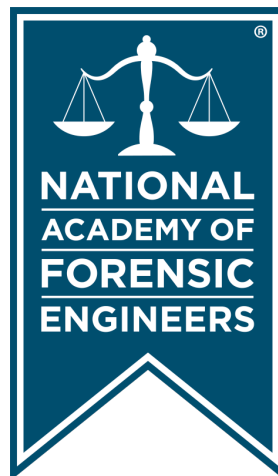


Journal of the  
**National**  
**Academy** OF  
**Forensic**  
**Engineers**<sup>®</sup>



<http://www.nafe.org>

ISSN: 2379-3252

Vol. 37 No. 1 December 2020

# Forensic Engineering Analysis of a Wheel Spindle Failure Due to Pre-Load and Fatigue

By David A. Danaher, PE (NAFE 703F)

## Abstract

*Typically, most vehicles equipped with non-powered wheels use a spindle that not only supports the weight of the vehicle but also allows the rotation of the tire. The rotation of the hub and wheel on the spindle is accomplished with the use of either a tapered or double row ball bearing. Bearings are mounted between the spindle and hub/wheel assembly, then secured with a castle nut set to a specified torque. Tapered bearings are chosen for this application because they are designed for applications where forces are generated radially (vertically) and axially (laterally) during use. Although tapered bearings are ideally suited for use in wheel and spindle assemblies, they must be installed properly to perform as designed. As part of that installation, the spindle nut must be properly torqued in order to apply a sufficient pre-load to the tapered bearings. Without the proper pre-load, the bearings can either generate too much friction or ride improperly on the spindle, generating forces that are not properly distributed. This paper will discuss the failure of a spindle and wheel assembly that experienced fatigue due to improper pre-load of the spindle nut.*

## Keywords

Tapered bearing, fatigue, failure, loading, wheel, spindle, pre-load, torque, axle, bending, stress, forensic engineering

## Background

The accident involving the tapered bearing failure occurred on a two-lane highway in a rural part of eastern Colorado. The equipment was a Case IH combine that was traveling northbound on the highway when the left rear tire and wheel detached from the vehicle. Following the detachment, the combine rolled onto its roof and came to rest on the roadway near the intersection with a county road. **Figure 1** shows the rest position of the combine. The scope of the investigation was to determine if the detached

wheel of the combine was a result of the accident or if it was the cause of the accident.

## Accident Site

In investigating the wheel assembly failure, the dynamics of the accident were analyzed to determine if any external influences may have contributed to the wheel separation. To that end, the accident site was inspected and documented.

In the area of the crash, the northbound highway is a



**Figure 1**  
Rest position of combine.

straight and level asphalt road that comes to an intersection with a county road. The highway has one northbound and one southbound lane. The road is bordered by asphalt shoulders followed by grassy terrain. The speed limit for this highway is 65 mph.

The accident site was inspected, surveyed, and scanned to document any remaining physical evidence as well as the geometry of the roadway. At the time of the inspection, numerous gouges and fluid deposits were visible on the road. The evidence at the scene was surveyed with a total station and scanned with a Faro Focus 3D Laser scanner. The Faro collected 65,525,091 data points that captured the geometry of the roadway, roadway markings, signage, physical evidence, and other features around the area of the incident<sup>1</sup>. The data from the site inspection was then used to create a scaled diagram of the accident site. The site data was supplemented with photogrammetric analysis<sup>2,3,4,5,6,7,8</sup> of the photographs taken shortly after the accident. **Figure 2** depicts an example of the author's photogrammetry analysis. The upper image is the original photograph; the lower image depicts the results of our analysis. **Figure 3** depicts the scene diagram overlaid with an aerial photograph. The diagram is oriented with north to the right.



**Figure 3**  
Scene diagram showing the physical evidence and the rest position of the combine.

### Case Combine

The Case IH Axial-Flow 8230 involved in this crash was a 2013 model year combine. A placard on the vehicle listed the unladen weight as 18,100 kg (39,904 lb). This agricultural equipment was equipped with Firestone 28L-26 tires on the rear and Deep Tread 23° tires on the front, which have a maximum speed of 25 mph and 30 mph, respectively. The tires on the vehicle were directional and intended to be mounted in a specific orientation. The front tires were mounted in the correct orientation. The rear tires were mounted backward, such that they rotated in the incorrect direction.

Directional tires are designed for traction/performance. For a combine, the design would be for traction purposes. When the tires are rotating in the correct direction, they would provide optimal traction since the combine is driven on soft soil and muddy conditions. Therefore, the incorrect direction of the tires did not contribute to the accident; however, it could be an indication that the combine had been recently serviced.

The Case combine utilizes rear axle hydraulic steering and has an optional top speed of 18.6 mph. **Figure 4** and **Figure 5** show the vehicle at the time of the inspection. The combine was scanned using a Faro Focus 3D Laser



**Figure 2**  
Camera matched rest position of the combine.



**Figure 4**  
Right side of combine.

scanner, which collected more than 5 million data points that accurately captured the geometry of the combine<sup>1</sup>. **Figure 6** shows the 3D scan of the vehicle.

### Accident Sequence

Having gathered all the evidence and geometry from the scene as well as the combine, the data was then

analyzed in a scaled environment. The gouge found in the roadway matched with the left-rear axle prior to the vehicle rolling over. Furthermore, the tire marks that run parallel to the gouge also matched the right-rear tire of the combine. The gouging could only occur with the left rear tire already separated from the vehicle and therefore did not separate as a result of the rollover. Based on the above, the following sequence was determined.



**Figure 5**  
Left rear corner of combine.



**Figure 6**  
Scanned three-dimensional model of the combine.

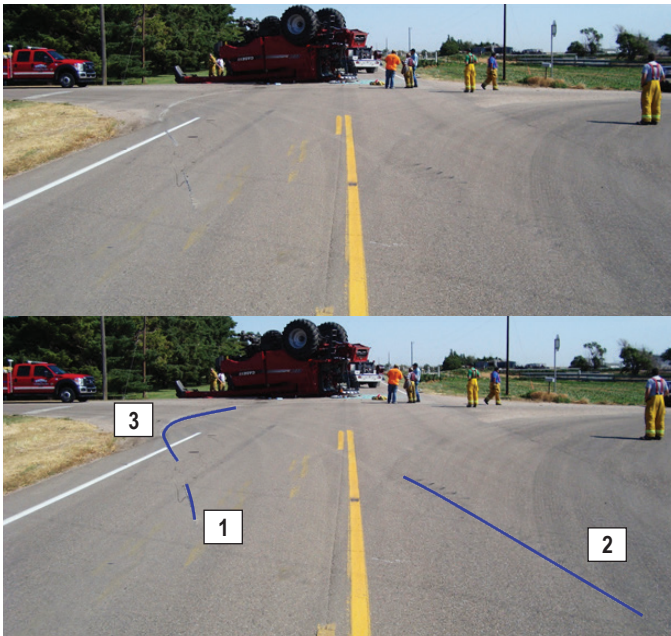


**Figure 7**  
Top image by police; bottom image highlights the physical evidence.

The combine was initially traveling north on the highway. The 14-ft-wide vehicle was likely occupying the shoulder and the entire (or nearly the entire) 11-ft-wide northbound lane. As the left-rear tire and rim detached, the vehicle was pulled to the left when the left-rear axle began gouging the southbound lane (labeled 1 in **Figure 7**). As the vehicle was pulled to the left, the right-side tires deposited yaw marks in the northbound lane (labeled 2 in **Figure 7**). The driver then steered to the right, causing the vehicle to yaw clockwise and curve to the right (as indicated by gouge number 3 in **Figure 7**). The combine then rolled one half time before coming to rest on its roof. **Figure 8** depicts the approximate motion of the combine through the physical evidence.

The evidence at the scene and the dynamics of the accident<sup>8,9,10,11,12,13,14,15</sup> showed that the failure and separation of the wheel assembly was not due to any environmental factors or interaction with another vehicle — and not as a result of, but rather the cause of, the rollover. Had the wheel separated from the combine due to an external force, there would have been significant damage to the tire and rim, which showed no evidence. Also, had the wheel assembly been attached before the rollover, there would have been no gouging left in the roadway prior to the rollover. Therefore, the wheel assembly separated prior to the rollover, requiring a deeper look at the damaged components of the wheel assembly (specifically the tapered bearings and spindle).



**Figure 8**  
Motion of the combine prior to rest along the physical evidence.

### Case Combine Wheel Assembly

The failed left rear tire and wheel were attached to the combine with a spindle, tapered roller bearings, washer, and a castle nut with a cotter pin. The spindle and hub are machined as one piece, with one end of the hub being bolted to the wheel, and the other end threaded with a provision for a cotter pin through a castle nut securing the hub and spindle assembly to the tractor. When assembled within the steering knuckle housing, the spindle is held in place and allowed to rotate via two tapered roller bearings. A tapered roller bearing uses hardened steel cylindrical bearings that are held in place by a steel cage. The tapered design allows the bearings to handle radial and axial loads. A washer is then placed on the inner bearing, and a nut is used to set the axial pre-load of the bearings. Once the pre-load is set correctly, a cotter pin is inserted through the

nut and spindle. **Figure 9** shows the general layout of the assembled components. The tire assembly would be to the left of the diagram.

As can be seen in **Figure 9**, the roller bearings are set at an angle relative to the spindle to allow for force along the axle. The relative angle of the bearing also generates thrust that will force the bearing off the spindle, requiring the use of a retention nut that is tightened to a specific torque, applying the proper amount of pre-load. The purpose of the pre-load is to maintain the location of the bearings relative to the spindle both radially and axially, maintaining the running position of the shaft and properly distributing the loading. The pre-load of the assembly is specified by the manufacturer.

One method for measuring the pre-load is to tighten the nut while measuring the axial displacement of the spindle with a dial indicator. The second method correlates the displacement to a specific nut torque that will set the proper pre-load. Improper pre-load can lead to excessive heat generation, increased frictional torque, and reduced bearing life due to fatigue.

To better illustrate how the spindle and bearing assembly is attached to the combine, **Figure 10** shows the right rear of the combine where the assembly is still intact. The image from **Figure 9** has now been overlaid onto the hub assembly in **Figure 11**.

At the time of the inspection, the left rear steering knuckle/housing were still attached to the rear axle. As depicted in **Figure 12**, the outer surface of the knuckle did not show signs of failure and was still attached to the combine.

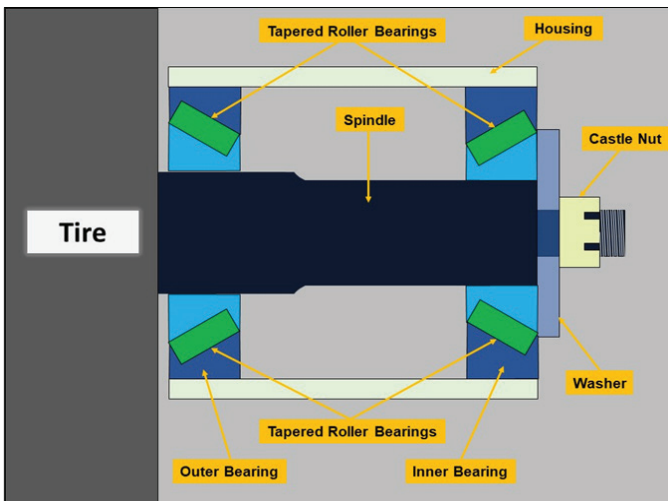


**Figure 9**

An example of a spindle and tapered bearing assembly.



**Figure 10**

Right rear tire and hub assembly.



**Figure 11**  
Right rear tire and hub assembly showing spindle and bearing diagram.

Additionally, the dust/grease cap was still attached to the inboard portion of the steering knuckle. At the time of this engineer's inspection, several components (such as the inner bearing, washer, and nut) were found inside the housing as well as an adequate amount of grease (see **Figure 13**). Within the steering knuckle housing, the tapered roller bearing, washer, castle nut, and cotter pin were removed and cleaned. **Figure 14** depicts these components cleaned as well as the dust/grease cap.

At the time of the inspection the left wheel was located next to the vehicle. The spindle, shown in **Figure 15**, was still attached to the wheel, covered in grease, and still had the outer tapered bearing seated on the spindle.

### Damaged Components

Inspection of the components revealed that the spindle, spindle threads, washer, and nut were damaged and showed signs of wear prior to the failure. The following



**Figure 12**  
Left and right images oriented with vehicle's front to the left and top, respectively.



**Figure 13**  
View inside left rear steering knuckle showing spindle components and grease.

outlines the damage exhibited by each component:

#### *Spindle Threads*

The diameter of the threaded portion of the spindle measures approximately 0.9 in. Examination of the spindle shows that the threaded portion where the castle nut attaches was damaged (**Figure 16**). The threads were damaged in two ways: the end portion of the threads was fractured off and remained in the castle nut, and the remaining threads were flattened around the circumference of the shaft.

#### *Castle Nut*

As shown in **Figure 17**, a portion of the threaded shaft



**Figure 14**

From left to right – castle nut, washer, inner bearing, and dust/grease cap.



**Figure 15**

Attached section of the spindle and outer bearing.



**Figure 17**

Nut, washer side.

is still attached to the nut, and there is damage to the surface of the nut that mates to the washer. The damage to the surface of the nut was due to the rotation of the nut relative to the washer and displaced/removed material from the mating surface. Furthermore, the damage and removal of the material to the nut would have increased the distance in the assembly, thereby decreasing the axial load, allowing more displacement of the bearing, and increasing misalignment in the assembly.

#### Washer

The washer in **Figure 18** was damaged with material displaced/removed on both sides from the contact with the inner bearing and the nut. The washer depicted in **Figure 18** shows damage from the rotation and impact damage of the washer relative to the bearing on the left and the nut on the right. The damage displaced some of the material of the washer, which is a softer

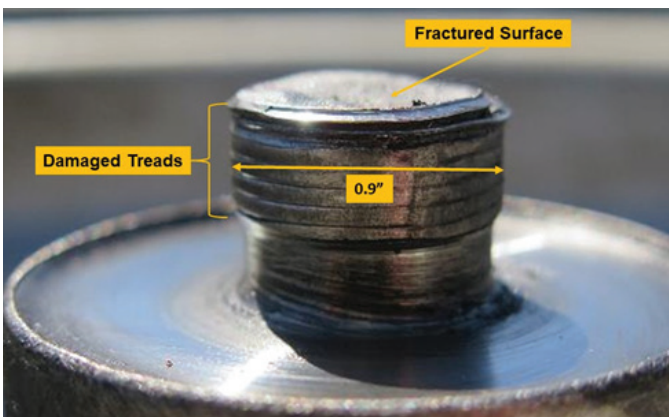


**Figure 16**

Spindle threads.



**Figure 18**  
Washer bearing side (left), nut side (right).

material than the bearing. A depression was made on both sides of the washer, increasing the amount of axial and radial movement of the spindle and also decreasing the pre-load. All three components — the washer, the tapered bearing, and the castle nut — were assembled on site and are shown in **Figure 19**.

### *Spindle Shaft*

The spindle measures approximately 2.50 in. in diameter and had visible signs of damage near the threaded end of the shaft. The damage was the result of the inner bearing race moving relative to the spindle. The damage to the spindle shaft as well as the described dimensions is shown in **Figure 20**. In this photograph, the area denoted by the yellow rectangle shows where the inner race of the

inner bearing was rotating and impacting on the spindle. The damaged area to the spindle outlined in yellow is approximately 1.50 in. in width, approximately 0.25 in. greater than the width of the bearing. Furthermore, at the bottom of the rectangle, there is also a depression from the spinning race that dug into the spindle. This damage to the spindle was consistent with the relative movement of the bearing on the spindle. On the right in **Figure 20**, material was also displaced over the surface where the diameter changes from the bearing landing to the threaded section, giving the end of the spindle a dished shape.

### *Inner Bearing*

The thickness of the bearing measures approximately 1.25 in. with an inner diameter of approximately 2.50 in. The inner bearing showed markings on the edge of the inner race from contact with the washer. The bearing shown in **Figures 21** and **22** shows the scratches to the race and the condition of the cylindrical roller bearings.

In the right image of **Figure 21**, marks can be seen from the bearing moving against the washer, causing abrasion marks. This indicates that the inner race of the bearing was allowed to move relative to the washer<sup>16,17</sup>. **Figure 22** depicts the rollers of the bearing. The faces of the roller bearings are smooth with no gouge or pitting marks evident as well as no discoloration, which would indicate that there was proper lubrication to the bearing at the time of the spindle failure<sup>17</sup>.



**Figure 19**  
Assembly of the tapered bearing, washer, and castle nut.

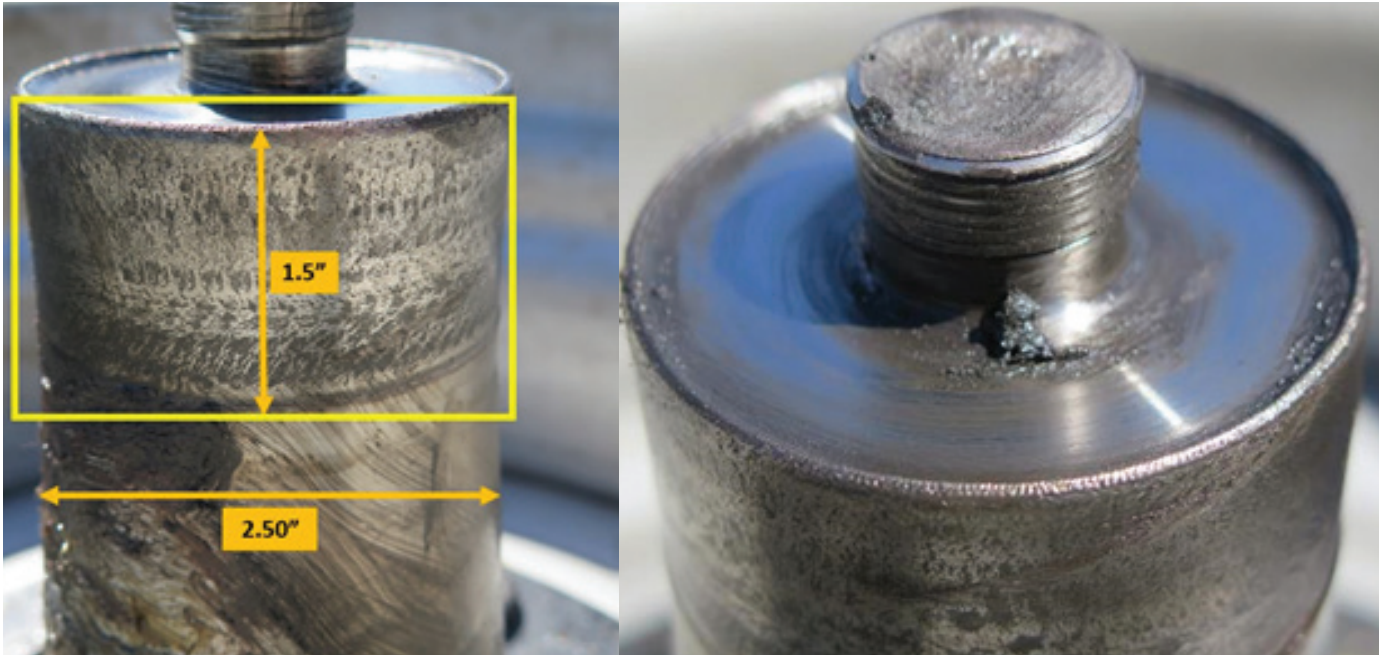


**Figure 20**

Spindle section attached to the separated wheel of the combine.



**Figure 21**

Scratch pattern on inner race edge.

### *Spindle Thread Failure*

The root cause of the spindle, bearing, washer, and nut moving independently of each other was the insufficient pre-load on the bearings<sup>18,19,20,21</sup>. The lack of pre-load resulted in insufficient frictional force between the components and allowed relative rotation of the mating parts. The lack of pre-load also allowed the increase in axial force from the weight of the combine, which results in a thrusting force toward the castle nut that should be applied perpendicular to the axel. Once the components started to move relative to each other, the washer and spindle began



**Figure 22**

Outer roller bearing.

to wear, further exacerbating the problem. The increased axial and radial motion increased the stress in the spindle thread area and generated an unintended moment about the threaded portion of the spindle. In the left image of **Figure 23**, the castle nut is properly tightened, and the tapered bearings are fully seated on the spindle. In the right image of **Figure 23**, the nut is now loose, allowing the inner bearing to unseat from the outer race and the spindle.

The movement of the inner bearing toward the threaded portion of the spindle places a moment not only on the smallest cross section of the spindle, but also on the greatest location of stress concentrations, namely the threads. **Figure 24** shows the moment placed on the threaded portion of the spindle and the corresponding forces as the spindle is allowed to freely move inside the housing.

Examination of the fracture surface shows that the threaded area was subjected to repetitive overloading and fatigue. For comparison, the fracture surface of the spindle thread is shown in **Figure 25**, and an example of a fracture surface that failed due to fatigue is shown in **Figure 26**.

In **Figure 25**, a relatively smooth area with beach marks can be seen as well as a rougher area with no beach lines. This is consistent with the example of a fatigue failure in **Figure 26**, specifically the presence of an area of fatigue and an area of overload.

The pattern on the nut end and the mating spindle (shown in **Figure 27** is consistent with unidirectional bending<sup>22</sup> where the force is applied from one direction as seen with the fatigue area making a horse-shoe shape

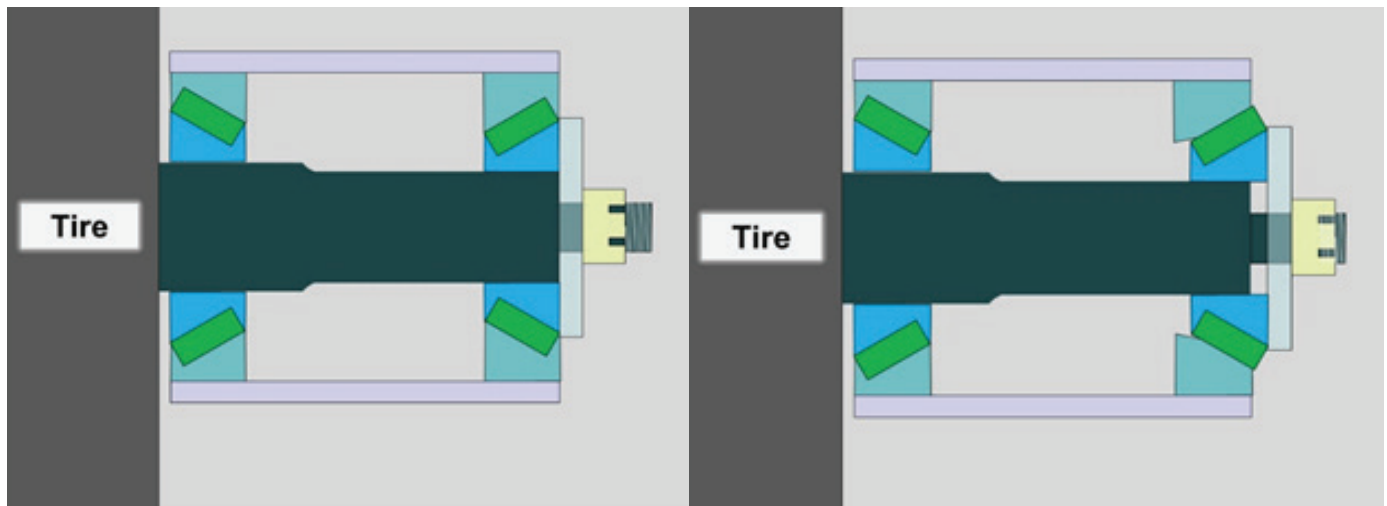


**Figure 23**  
(Left image) properly tightened nut – (right image) improperly tightened nut.

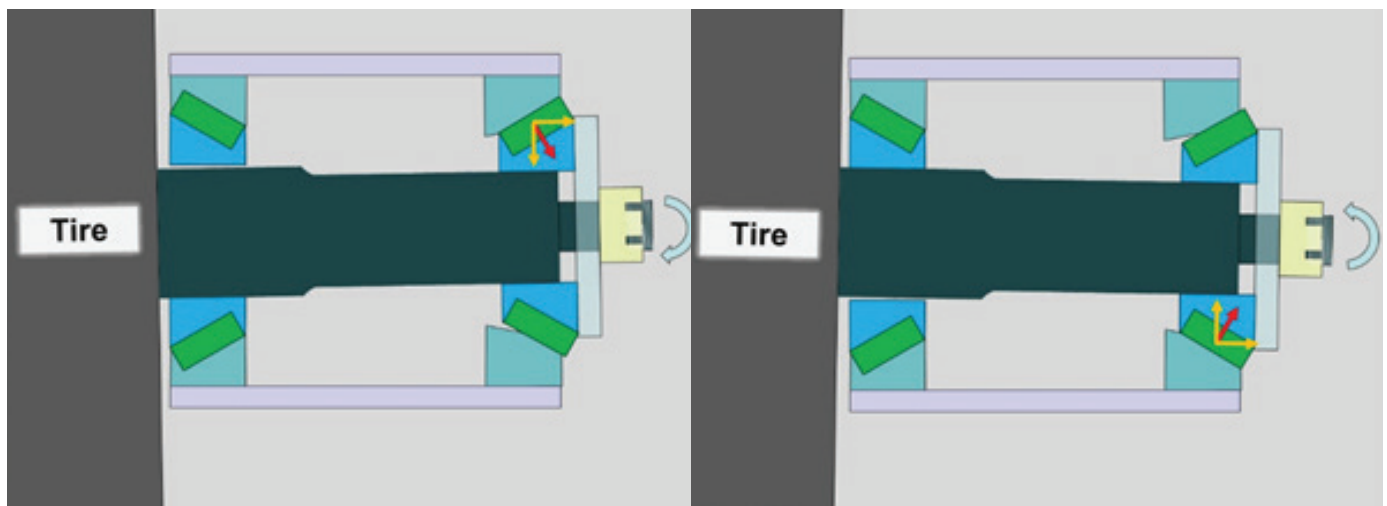


**Figure 24**  
Moment placed on the threaded portion of the spindle.

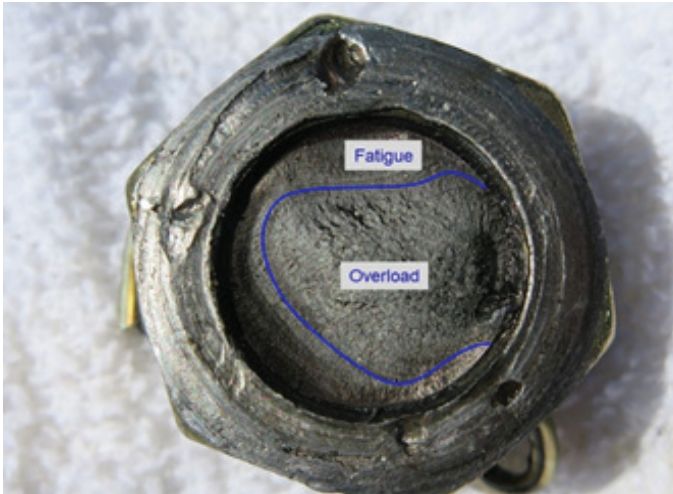


**Figure 25**  
Fracture surface on castle nut.

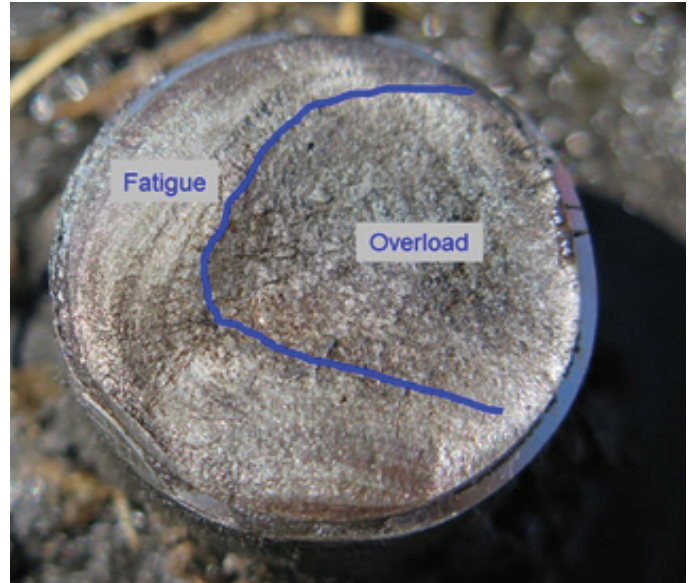


**Figure 27**  
The fatigue horse-shoe pattern shown on spindle.

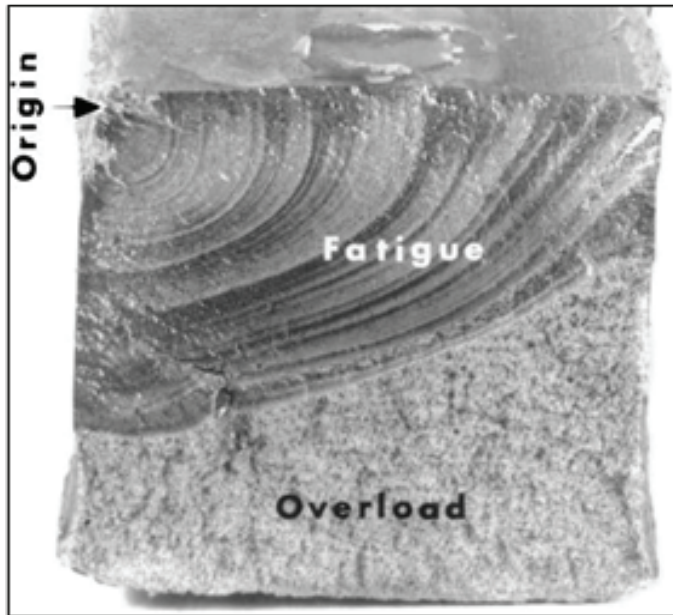


**Figure 26**  
Example of fatigue<sup>21</sup>.

around the overloaded area. **Figure 28** shows an example of unidirectional bending from the ASM handbook<sup>22</sup>.

### Conclusion

The insufficient pre-load allowed the inner race of the inner bearing to move on the spindle, causing damage to the spindle and allowing the spindle to move in an axial and radial direction. This further decreased the pre-load, which allowed the washer to start rotating relative to the bearing and nut. This rotation damaged the washer and further increased the amount radial and axial motion.

The increased axial and radial motion increased the

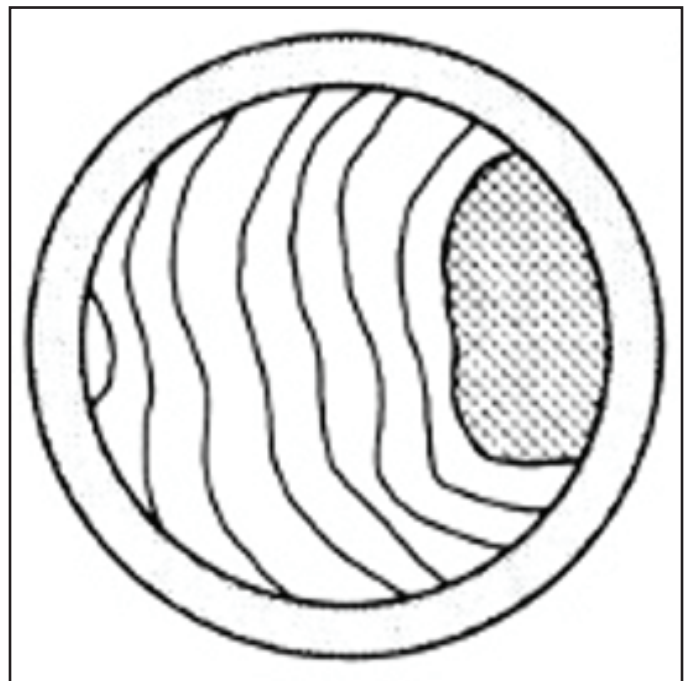


**Figure 28**  
Unidirectional bending – ASM Handbook<sup>22</sup>.

stress in the spindle thread area and generated an unintended moment about the threaded portion of the spindle. The movement of the inner bearing toward the threaded portion of the spindle placed a moment not only on the smallest cross section of the spindle, but also on the greatest location of stress concentrations, namely the threads.

The insufficient pre-load allowed a portion of the load on the spindle to be distributed to the smaller cross-sectional

area of the threaded section. The correct pre-load allows for the proper positioning of the bearings on the spindle and by extension the proper distribution of the force. When the nut is not tightened to the correct position, the bearings inherently want to migrate out as far as they are allowed. In this instance, the bearing traveled toward the smaller threaded cross-sectional area, which applied an unintentional bending moment to the weakest part of the spindle. The threaded section was not designed to have a bending moment applied to it; the threaded section was simply there to keep the bearing in place. However, when the nut was not tightened sufficiently, the load from the combine on that axle created a bending moment.

A bending moment creates a stress on the threaded section that is a function of the load carried on that axle and the cross-sectional area of the spindle. The formula(s)<sup>23</sup> to determine stress is shown in equations 1, 2, and 3.

$$\text{Eq. 1: } M=Fx$$

$$\text{Eq. 2: } I= (\pi r^4)/4$$

$$\text{Eq. 3: } \sigma=(M c)/I$$

The cross-sectional area of the spindle is approximately 4.9 in.<sup>2</sup> compared to approximately 0.64 in.<sup>2</sup> of the threaded portion — more than seven times smaller than the spindle. When calculating the stress in the spindle compared to the stress in the threaded section, the stress is increased by 25 times.

The stress in the threaded portion of the spindle exceeded the fatigue limit of the material over time and eventually led to a sudden fracture, which allowed the wheel to separate from the combine — and the combine to subsequently rollover.

*Acknowledgments: I would like to thank Gray Beauchamp, PE, for his contribution in investigating this case. Mr. Beauchamp provided much of the analysis in vehicle dynamics and accident reconstruction.*

## References:

1. N. Carter, Evaluation of the Accuracy of Image Based Scanning as a Basis for Photogrammetric Reconstruction of Physical Evidence, 2016-01-1467, Warrendale: Society of Automotive Engineers, 2016.
2. R. M. Brach, Vehicle Accident Analysis and

Reconstruction Methods, Warrendale: Society of Automotive Engineers, 2005.

3. C. Chou, Image Analysis of Rollover Crash Tests Using Photogrammetry, 2006-01-0723, Warrendale: Society of Automotive Engineers, 2006.
4. Steve Fenton, Accident Scene Diagramming Using New Photogrammetric Technique, 970944, Warrendale: Society of Automotive Engineers, 1997.
5. Steve Fenton, Using Digital Photogrammetry to Determine Vehicle Crush and Equivalent Barrier Speed (EBS), 1999-01-0439, Warrendale: Society of Automotive Engineer, 1999.
6. James Funk, Occupant Ejection Trajectories in Rollover Crashes: Full-Scale Testing and Real World Cases, 2008-01-0166, Warrendale: Society of Automotive Engineers, 2008.
7. William Neal, Photogrammetric Measurement Error Associated with Lens Distortion, 2011-01-0286, Warrendale: Society of Automotive Engineers, 2011.
8. Nathan Rose, A Method to Quantify Vehicle Dynamics and Deformation for Vehicle Rollover Tests Using Camera-Matching Video Analysis, 2008-01-0350, Warrendale: Society of Automotive Engineers, 2008.
9. K. Baker, Traffic Collision Investigation, Evanston: Northwestern University Center for Public Safety, 2001.
10. G. Beauchamp, Determining Vehicle Steering and Braking from Yaw Mark Striations, 2009-01-0092, Warrendale: Society of Automotive Engineers, 2009.
11. R. Brach, Vehicle Accident Analysis and Reconstruction Methods, Warrendale: Society of Automotive Engineers, 2005.
12. J. Daily, Fundamentals of Traffic Crash Reconstruction, Jacksonville: Police Technology and Management, University of North Florida, 2006.
13. N. Rose, Factors Influencing Roof-to-Ground

Impact Severity: Video Analysis and Analytical Modeling, 2007-01-0726, Warrendale: Society of Automotive Engineers, 2007.

14. N. Rose, Development of a Vehicle Deceleration Rate Approach to Rollover Crash Reconstruction, 2009-01-0093, Warrendale: Society of Automotive Engineers, 2009.
15. L. Fricke, Traffic Accident Reconstruction, Warrendale: Society of Automotive Engineers, 2010.
16. SKF, "Principles of Rolling Bearing Selection," SKF, 2018. [Online]. Available: 16. <https://www.skf.com/group/products/bearings-units-housings/principles/bearing-selection-process/bearing-type-arrangement/arrangements-and-their-bearing-types/index.html>. [Accessed 2018].
17. Timken, "Timken Bearing Damage Analysis with Lubrication Reference Guide," Timken, North Canton, 2015.
18. E. Avallone, "Mark's Standard Handbook for Mechanical Engineers 10th Edition," McGraw-Hill, 1996.
19. Morton & Control, "NSK Rolling Bearings Preload," NSK, Japan, 2018.
20. R. Norton, Machine Design an Integrated Approach, Prentice-Hall, 1996.
21. N. Dowling, Mechanical Behavior of Materials, 4th Edition, Pearson Education, 2013.
22. ASM, ASM Handbook Committee, Fractography, Vol 12, Visual Examination and Light Microscopy, pg. 118, ASM International, 1987.
23. M. Lindeburg, Mechanical Engineering Reference Manual for the PE Exam, Eleventh Edition, Belmont: Professional Publications, 2001.